MNRAS 000, 1–9 (2024) Preprint 5th May 2025 Compiled using MNRAS LATEX style file v3.3

Seven Decades of Quasar Photometry: Paper II - A Detailed Structure Function Analysis of 7-DQ

Harry Rendell-Bhatti,[1] Andy Lawrence,[1]
[1]*Institute for Astronomy, University of Edinburgh, Royal Observatory, Blackford Hill, Edinburgh EH9 3HJ, UK*

Accepted XXX. Received YYY; in original form ZZZ

ABSTRACT

Key words: quasar – structure function – ensemble

1 INTRODUCTION

The variability of quasars is an important diagnostic of the the physical process generating their emission, potentially giving insight into otherwise unresolvable regions, with for example the observation of optical variability on timescales of $\sim$ months being incompatible with simple accretion disc models (eg oldrefs, Lawrence 2012, 2018). It has been clear from the earliest observations that quasars do not exhibit either periodic variability or purely random noise, but something more like flicker noise, with larger amplitude variability on longer timescales (e.g. Press 1992). It then becomes of interest to characterise and quantify the dependence of amplitude on timescale. This can be done in a variety of ways, for example using the power spectrum or the autocorrelation function, but the technique that has become most popular for quasar studies is the *Structure Function (SF)*, which roughly speaking measures the variance of the difference of pairs of measurements separated by a given time lag (e.g. Simonetti et al 1985, Hook et al 1994, de Vries et al 2005, MacLeod et al 2012, Kozlowski et al 2016). The SF provides a robust means to quantify variability of irregular and sparse time series. (What was that paper arguing SF not a good choice?)

Starting with Kelly et al (2009), it has been popular to assume that the SF of quasars is best modelled as a *Damped Random Walk (DRW)*, but there is no proper physical model of the origin of variability to justify this. The DRW is not really a model, but rather a convenient mathematical characterisation. However, in any physical model, we know that the amplitude of variability cannot continue to increase to indefinitely long timescales; one advantage of the DRW characterisation is then that it has a knee timescale τ_{DRW} beyond which the SF transitions to being flat, i.e. white noise on long timescale. Such a timescale might, for example, be identified as being connected with the outer edge of the radiating region, and so be a key physical clue. Fitting a DRW to the SF of an individual quasar gives a number which can potentially be identified as a characteristic timescale, which could be correlated with other properties (refs).

Typical quasar light curves are poorly and thinly sampled, so that derived SFs can have significant systematic errors and biases. It has become common therefore to calculate the SF of large quasar samples, treated as an ensemble, on the assumption that all the quasars in the ensemble have on average the same SF. As well as beating down the noise on the typical amplitude of magnitude differences, the range of redshifts and so time dilations conveniently fills in the range of time lags. Although some such studies (eg MacLeod et al 2012) have claimed evidence for a turnover in the SF at long timescales, others have argued that the SF is a pure power law over decades of lag timescale (eg De Vries et al 2005, Morganson et al) and so not consistent with a DRW form.

Meanwhile, it may not be reasonable to assume that all objects in the ensemble are the same. There is clearly evidence that variability depends on some combination of Luminosity, Black Hole Mass, and Eddington ratio (for example Hook et al 1994, de Vries et al 2005, MacLeod et al 2010). Our aim in this paper is to revisit and improve our understanding of these issues - the true shape of the SF, and it's dependence on quasar properties - using the largest sample of long quasar light curves so far.

In Paper I, we defined the 7-DQ sample - 526,356 spectroscopically confirmed quasars from SDSS DR14 - and assembled photometry from multiple surveys spread over seventy years, reducing the photometry to a common system. The number of epochs per quasar varies considerably, but is typically around 200-600, with a majority of these coming the ZTF survey. We also compiled a control sample of 399,922 stars, and a (very large) dataset of all pairwise magnitude differences, for the convenience of later analysis.

As well as describing the construction and testing of the 7-DQ sample, Paper I presented some initial science results - testing recent claims of a systematic downward drift in average quasar magnitudes, the first ever analysis of the kurtosis and skewness of quasar variability as a function of lag, and a preliminary analysis of the SF. We described our improved techniques for estimation of the SF, and showed the resulting ensemble SF in the r-band. This seems to be a pure power-law over four decades of lag timescale, and strongly inconsistent with a DRW form. However, we also showed the SF found for a bright subset of the 7-DQ sample, with $g < 20$. This closely matches the SF of the whole sample over most of the timescale range, but shows some steepening at shorter timescales. This may reflect more reliable photometry in the brighter sample, but there is no sign of a similar effect in the star sample. On the other hand, short timescale steepening may be because the brighter quasars are systematically more luminous.

In this paper, we present a more complete analysis of the SF. We start in Section 2 by summarising the techniques we used to estimate

the SF, which are explained in more detail in Paper I. In Section 3 we present the resulting SF in g, r and i bands, characterise its shape, and compare what we have found to the results of previous workers. In Section 5 we divide our sample into sub-ensembles, based on Luminosity, Black Hole Mass, and Eddington ratio, and examine how the shape and amplitude of the SF varies with those properties. In Section 6 we tackle the issue of dependence on quasar properties in a different way, by estimating the SF for individual quasars, then correlating the amplitude of the SF with Luminosity, Black Hole Mass, and Eddington ratio as a function of time lag. Finally in section 7 we discuss these results, asking in particular whether the DRW interpretation can be rescued, and what the alternatives may be.

2 CALCULATION OF THE STRUCTURE FUNCTION

Here we summarise our definition of the SF, and the methods used to estimate the SF of an ensemble. More detail on the techniques is given in Paper I. In Appendix A we describe the various subtly different definitions that have been used in the literature in the past. In Appendix B we examine how much difference it makes working in magnitudes as opposed to fluxes. (Brief answer: not much).

2.1 SF definition

For each quasar we have a set of magnitudes m, with photometric error σ, at absolute times t, including measurements from different surveys, reduced to a common system as described in Paper I. We then take all possible pairs of measurements at times t_i and t_j and form the magnitude differences Δm_{ij} and rest frame time lags $\Delta t = (t_j - t_i)/(1+z)$, where z is the quasar redshift. We wish to correct for the contribution of photometric error to the observed variability, and so estimate the *Intrinsic Structure Function* as

$$\mathrm{SF_{int}}(\Delta t) = \sqrt{\frac{1}{N(\Delta t)} \sum_{j<i} (\Delta m_{ij}^2 - \sigma_i^2 - \sigma_j^2)}, \quad (1)$$

where the sum runs over the $N(\Delta t)$ epochs.

2.2 Ensemble SF

Because we are using magnitude differences and relative time lags, we can combine all the $(\Delta m, \Delta t)$ pairs for an ensemble of quasars. The SF for an ensemble is identical except for an additional sum:

$$\mathrm{SF_{int,ensemble}}(\Delta t) = \sqrt{\frac{1}{N(\Delta t)} \sum_k \sum_{j<i} (\Delta m_{ij,k}^2 - \sigma_{i,k}^2 - \sigma_{j,k}^2)}, \quad (2)$$

where k denotes the index of the quasar.

2.3 Variance weighted estimate

Subtracting photometric error in the manner indicated by eqn. (1) can lead to negative values of the SF, especially on short timescales where the intrinsic variability is small. One possible solution is to restrict the dataset to points with small errors. However, this wastes information. We therefore weight values of Δm^2 by their inverse-variance, which is common practice for optimal averages. We define weights for a given i, j pair, indexed by k, as

$$w_k = \mathrm{Var}[\mathrm{SF}^2(\Delta t)]^{-1} = \frac{1}{2}(\sigma_i^2 + \sigma_j^2)^{-2}, \quad (3)$$

and then calculate the variance weighted structure function as

Filterband	β	α_1	α_2	α_3
g	0.361 ± 0.003	0.019 ± 0.003	0.100	0.528
r	0.355 ± 0.004	0.018 ± 0.004	0.092	0.473
i	0.418 ± 0.007	0.011 ± 0.007	0.075	0.517

Table 1. Results from fitting the ensemble structure function with a single power law to the three bands. The amplitudes tabulated are in magnitudes, and are for a rest frame timescale of 1 day, 100 days, and 10,000 days respectively.

$$\widehat{\mathrm{SF}}(\Delta t) = \sqrt{\frac{\sum_k \mathrm{SF}_k^2(\Delta t) \cdot w_k}{\sum_k w_k}}. \quad (4)$$

The errors on these values are given by

$$\sigma_{\widehat{\mathrm{SF}}} = \left(\sum_k w_k \right)^{-1/2}. \quad (5)$$

A derivation of these quantities is given in Paper I, where we also show that this method gives a much smoother SF and more reliable than that calculated by the simple method of eqn. (1). This method is what we use throughout the rest of this paper, where we refer to this quantity simply as "the structure function".

3 THE MULTI-BAND ENSEMBLE STRUCTURE FUNCTION

In this section we look at the SF calculated from the full sample, for each of the g, r and i bands, examine it's shape, and then compare to work from previous studies.

3.1 The shape of the structure function

In Fig. 1 we show the r band structure function calculated from our sample, together with the SF calculated for the star control sample. (Structure functions for the other bands are shown in Appendix C). On timescales $\Delta t > 10$ days, the quasar ensemble structure function appears to follow a single power law (SPL) up to the longest timescales of $\Delta t \sim 10^4$ days. Therefore, we fitted SPLs of the form

$$\mathrm{SF_{SPL}}(\Delta t) = \alpha \Delta t^{\beta} \quad (6)$$

to each band, over these timescales. The r and i band structure functions continue to follow a SPL (within error) even on the longest timescales, indicated by the right-most points. The final point of the g band structure function deviates from an SPL. However, relatively fewer pairs are used in this final bin (10^4, compared to a mean 10^8 pairs for all bins) and therefore it is less reliable.

Note that α is units of magnitudes, and Δt in units of rest-frame days. The amplitude α is therefore the size of SF on a timescale of 1 day. Of course this is not where most of the data constraining the fit is. Table 1 shows the fitted results, giving amplitudes at 1, 100, and 10,000 days. To first order, the SF at g, r and i are the same, with some evidence that the i-band SF is steeper and of lower amplitude. On a timescale of 1, 100, and 10,000 days, quasars typically vary in flux by $\sim 2\%$, 10%, and 60% respectively.

A power law of slope $\beta \sim 0.35$ over several decades seems clearly incompatible with a Damped Random Walk (DRW). A DRW should show a SF of the form

$$\mathrm{SF}(\Delta t) = \mathrm{SF}_\infty \left(1 - e^{\Delta t/\tau}\right)^{1/2}. \quad (7)$$

where SF_∞ is the long timescale asymptotic value, and τ is the knee timescale (eg Macleod et al 2010, Kozlowski 2016, Lawrence-PiP).

On the log-log plot, this has a short timescale slope of $\beta = 0.5$ and a long timescale slope of $\beta = 0$ - in other words, at short timescales the behaviour is like a simple random walk, and on long timescales, like white noise. There is of course a gradual roll-over. Is it that we happen to be observing on timescales corresponding to the roll-over region? The consistency of the observed $\beta = 0.35$ slope over several decades is not consistent with this idea. Given our errors, the range over which the apparent logarithmic slope could be consistent with what we see is less than a decade. Of course, if *individual* quasars do have variations described by a DRW, their SFs could have many different amplitudes and knee timescales, so that the net ensemble SF resulting from mixing them could mimic a power-law slope. In section 7 we test this idea with a simple simulation, and in section 5 we split our sample into sub-ensembles, based on quasar properties, to look for signs of such differences.

3.2 Comparison to previous work

There have been many massive variability studies over the years. A summary of results on the shape of the SF is presented in Table 2. Here we we will concentrate on comparing our ensemble structure function with three particularly comprehensive studies, which calculate the ensemble structure function on long timescales. These studies are de Vries et al. (2005), MacLeod et al. (2012), and Morganson et al. (2014) which we will refer to as dV05, M12, and Mo14, respectively, hereafter. The results of de Vries et al. (2005) and Morganson et al. (2014) are plotted along with our r-band result is Figure 1, with the other bands compared in Figure C1. M12 used a sample of 33,881 quasars over a baseline of 50 years in the observer frame by using POSS and SDSS plate data. dV05 used a similar sized sample, 35,165 quasars, with photometry again from POSS and SDSS such that their baseline was also 50 years. Mo14 compared SDSS and Pan-STARRS photometry for 10^5 over a baseline of 10 years. These studies have some of the longest baselines to date, and while more recent studies have expanded their sample size or number of observations per object, none have compared the most recent observations against historic plate photometry to push to new temporal baselines.

dV05 found that their ensemble structure function follows a SPL with a slope of $\beta = 0.30 \pm 0.01$ and no sign of a turnover (i.e., no break in the SPL) up to ~40 years in the rest-frame. Consequently, they concluded that there is no single preferred characteristic timescale for the quasars, but instead most likely a continuum of timescales. M12 covered a much larger range of Δt by using repeat imaging of quasars in SDSS Stripe 82. Given the overall shape of their structure function, in particular the hint of a turnover at long time-lags, they concluded that their structure function is consistent with that of a damped random walk. The baseline of Mo14 does not extend as far as the other two studies, but they show a consistent SPL on all observed timescales, with slopes of $\beta_g = 0.251 \pm 0.004$, $\beta_r = 0.275 \pm 0.004$, and $\beta_i = 0.277 \pm 0.005$.

Comparing our result with the results of dV05 and M12, we see that all structure functions are in agreement for $10^2 - 10^3$ days. Remarkably, our r-band structure function is strikingly similar to dV05 $\Delta t > 10^3$, despite using mostly different data. However, we estimate significantly more variability than M12 on timescales $\Delta t < 10^2$ days. We suspect that it is because we are more likely to catch short-lived outburst events, given that ZTF has a high cadence. These outburst events often involve dramatic changes in magnitude and therefore increase the structure function on these timescales. Additionally, M12 uses the interquartile range (IQR) to calculate their structure function (see Equation M12), which reduce the effect of such outbursts on their results. Mo14 report a higher structure function amplitude in all three bands compared to our results and the other studies, which could be due to residual photometric noise that has not been properly subtracted. This also leads to a flatter structure function, which is the cause of their significantly flatter SPL slopes.

The long-term behaviour of the structure function (i.e., on timescales $\Delta t > 20$ years) is a contentious topic, but the literature involving its calculation tend to follow a common theme: the structure function initially grows as an SPL on timescales up to 1–3 years, then does one of two things based on the subsequent data points, which are often only a few. Either the structure function breaks from the SPL and starts to turnover at some characteristic timescale, often denoted τ (see e.g., MacLeod et al. 2012; Sesar et al. 2006; Stone et al. 2022; Voevodkin 2011), or, the structure function continues to follow the SPL on all observed timescales (see e.g., Hawkins 2002; de Vries et al. 2005; Vanden Berk et al. 2004; Morganson et al. 2014). A few studies claim that their data is unable to discern between the two, usually due to uncertainties (see e.g., Li et al. 2018).

The quasar structure function cannot continue to follow a SPL for all time-lags. Therefore, variability studies often claim a characteristic timescale indicated by turnover, which would solve the issue of 'infinite power at infinite time-lags'. Since the shape of the structure function is not usually well constrained on the upper bound of time-lags of any particular study, one can convince themselves that a turnover is visible on those time-lags if the final few data points start to drop. Therefore, it is important to remain agnostic and acknowledge that a characteristic timescale could be orders of magnitude longer than the timescales we are currently able to observe.

Many studies that claim a turnover fit the DRW structure function to their data (see e.g., Sesar et al. 2006; MacLeod et al. 2012; Stone et al. 2022). The DRW model is attractive because it plateaus for $\Delta t \gg \tau_{\rm DRW}$, where $\tau_{\rm DRW}$ is the characteristic DRW timescale, effectively preventing the light curve from reaching arbitrary magnitudes. However, for $\Delta t \ll \tau_{\rm DRW}$, the DRW has a slope of $\beta = 0.5$ which is much too steep for the majority of slopes seen in observational data.

4 STRUCTURE FUNCTION ASYMMETRY

dV05 found a small but clear difference in the structure function for positive and negative variations. In this section we look for this effect in our dataset. While the structure function measures the absolute overall variance, asymmetries between the rising and falling parts of the light curve can be investigated by separating the fluctuations into positive and negative changes, computing their respective structure functions and comparing them. We use the same methods as described in Section 2, but collect positive and negative values of Δm_{ij} separately, together with their corresponding errors. For convenience we refer to the resulting SF values as SF+ (dimming) and SF-(brightening).

The r-band results are shown in Fig. 2, with the other bands shown in Figure C2. (The other bands show similar behaviour.) Note that the linear value of the SF is plotted in this case. The stars do not show a significant difference between SF+ and SF-, which is reassuring. For the quasars, SF+ and SF- are identical at timescales less than a year. From 1 to ~20 years, SF->SF+, but the SFs then cross over so that on the longest timescales SF+ >SF-. This behaviour is consistent across all three bands, and implies that the timescales for brightening and dimming are different, with brightening favouring timescales ~ 10 years, and dimming favouring timescales > 30 years. Since SF+ and SF- are each an ensemble of the entire quasar sample, it is likely that there are a range of timescales, with the ones quoted here being an average.

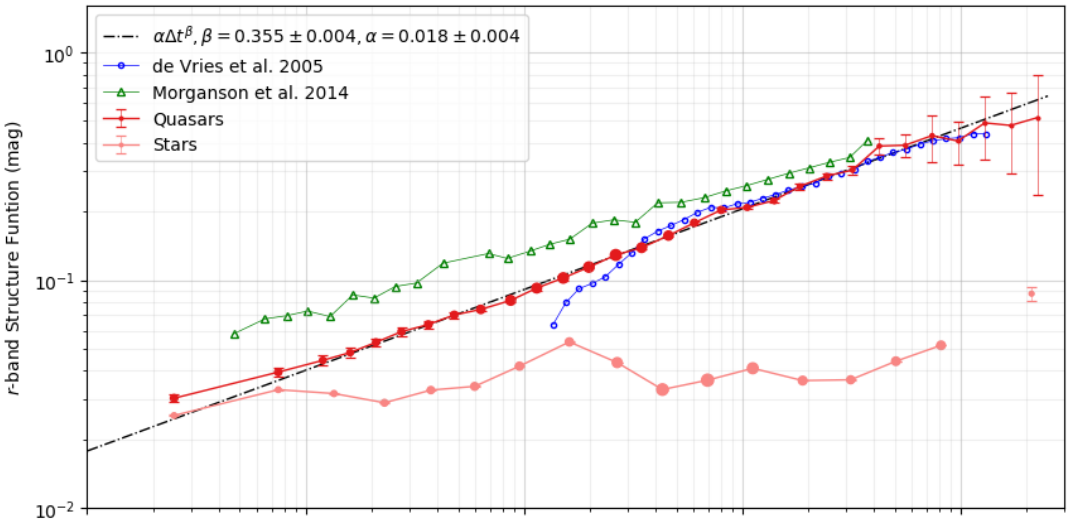

Figure 1. Ensemble structure function for the quasars and stars in the r band. (SF results for all of g, r and i bands are shown in Appendix C). The size of the points represents the relative number of points in the bin. The black dot-dashed line represents an SPL fit to the quasar structure function data points for $\Delta t > 10$ days, with the slope shown in the legend. Comparison data from de Vries et al. 2005, and Morganson et al. 2014 are overplotted. A few points are omitted for the ensemble star structure function, as the photometric errors are greater than the observed variability.

Table 2. Summary of recent massive variability studies that report ensemble structure function slopes

Authors	Bands	$N_{\rm obj}$	Δt [yr] observer frame	SF slope β
Hawkins 2002	Schmidt plates U, B, V, R, I	400	24	0.20 ± 0.01
de Vries et al. 2005	POSS SDSS g	31,165	50	0.30 ± 0.01
Vanden Berk et al. 2004	SDSS g, r, i	~25,000	2	g: 0.293 ± 0.030 r: 0.336 ± 0.033 i: 0.303 ± 0.035
Voevodkin 2011	SDSS g	7,562	10	~0.33 (for $\Delta t > 42$ days)
MacLeod et al. 2012	SDSS u, g, r, i, z	33,881	20	0.40 (for $\Delta t > 42$ days)
Morganson et al. 2014	SDSS, PS g, r, i, z	~100,000	10	g: 0.251 ± 0.004 r: 0.275 ± 0.004 i: 0.277 ± 0.005
Li et al. 2018	SDSS, PS g, r, z	119,305	15	0.254 ± 0.011
This work	UKST & POSS plates SDSS, PS, ZTF g, r, i	~500,000	70	g: 0.361 ± 0.003 r: 0.355 ± 0.004 i: 0.418 ± 0.007

These results are consistent with those of dV05, but stronger and clearer. They discussed a possible shot noise model to explain the asymmetry. In Section 7 we will discuss possible interpretations further.

5 DEPENDENCE OF THE STRUCTURE FUNCTION ON QUASAR PROPERTIES

Many simple correlations between variability and various physical quasar parameters have been known for several decades. These relationships from early studies are summarised by **?**, Helfand et al. (2001) and Lawrence 2016. Some of the early studies show a clear anticorrelation between variability and luminosity (see e.g., Angione & Smith 1972; Hook et al. 1994; Cristiani et al. 1997; Vanden Berk et al. 2004). However, luminosity is itself dependent on black hole

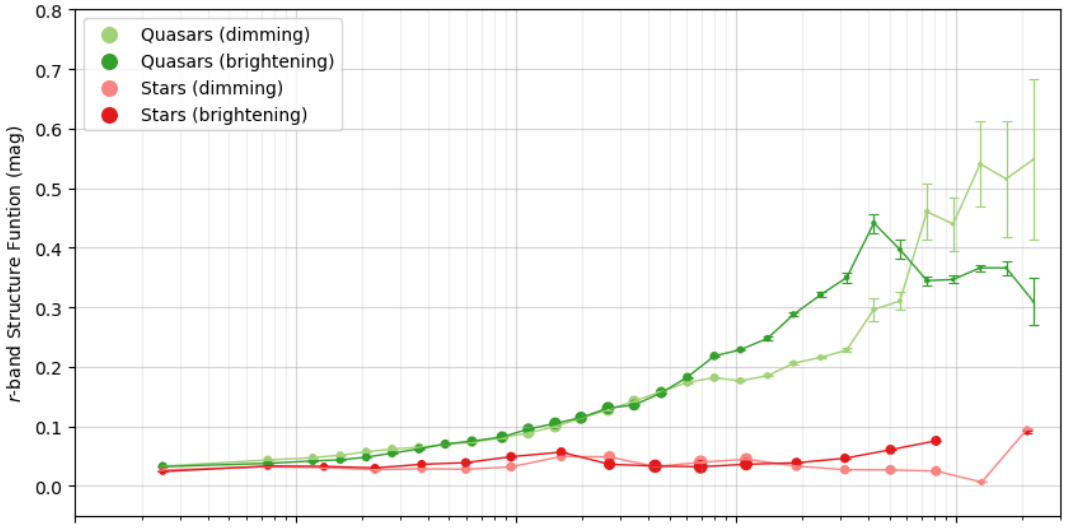

Figure 2. Positive and negative structure functions plotted for the quasar and star population in the g band.(SF results for all of g, r and i bands are shown in Appendix C) Fluctuations that involve brightening are illustrated with opaque points, while those representing dimming are in translucent points.

mass and accretion rate (quantified as the Eddington ratio). Recent studies have shown a statistically significant anticorrelation between variability and Eddington ratio (see e.g., Kelly et al. 2009; MacLeod et al. 2010; Zuo et al. 2012; Kelly et al. 2013; Simm et al. 2016; Rakshit & Stalin 2017; Sánchez-Sáez et al. 2018; Lu et al. 2019), but whether there is a relationship between variability and black hole mass is a debated issue. Positive correlations were found by Wilhite et al. (2008); MacLeod et al. (2010), and Lu et al. (2019), while negative correlations were found by Kelly et al. (2009) and Kelly et al. (2013). No clear correlations were reported by Zuo et al. (2012); Simm et al. (2016); Rakshit & Stalin (2017), and Li et al. (2018). Arévalo et al. (2023) state that these conflicting results can be reconciled when considering that these correlations depend on the timescale of observed variability.

We take two complementary approaches to studying the dependence of variability on quasar properties. (1) In this section, we divide the whole dataset into subensembles based on quasar properties and calculate the SF for each subensemble. (2) In the following section, we estimate the SF amplitude for each quasar individually, and then correlate these values with quasar properties.

We will focus on three key properties: bolometric luminosity, $L_{\rm bol}$, black hole mass, $M_{\rm BH}$, and Eddington ratio, $n_{\rm Edd} = L_{\rm bol}/M_{\rm BH}$. It has long been debated which of these properties is the main driver of variability. By grouping quasars by these properties and computing their respective structure functions, we are able to characterise the shape of the structure function with quasar properties, and determine which of these have the greatest impact on the amplitude of variability at different timescales.

5.1 Defining subensembles

We use values of $L_{\rm bol}$, $M_{\rm BH}$, and $n_{\rm Edd}$ from the DR16 catalogue of quasar properties provided by Wu & Shen (2022). We begin by cross-matching our quasar sample to obtain properties for 296,868 quasars. For each property p, we divide the quasars into groups, based on the the frequency distribution for that property, $N(p)$. We find the mean μ_p and standard deviation σ_p, and then generate the

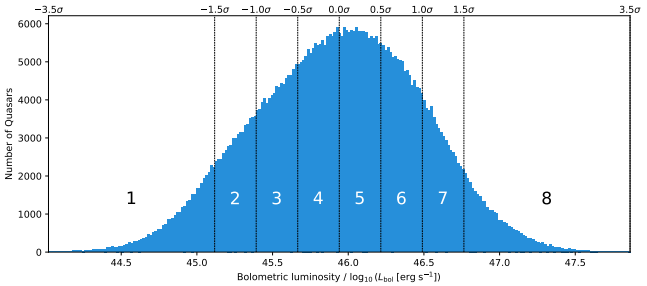

Figure 3. Distribution of bolometric luminosities within our quasar sample. The numbers in each rectangle denote which group the quasars belong to.

Z-score for each quasar q:

$$Z_{q,p} = \frac{x_{q,p} - \mu_p}{\sigma_p} \tag{8}$$

Using the Z-score, we proceeded to bin the quasars into 8 groups based on values of $Z_{q,p}$. An example using bolometric luminosity is shown in Figure 3. The central bin edge is on the mean of the distribution, and successive bin edges lie at multiples of 0.5σ. Note that the extremal bins have outer edges placed at $\pm 3.5\sigma$ such that their width is instead 2σ. This was done to ensure that the two bins covering the tail ends of the distribution have a similar number of quasars to those closer to the mean. This produces a total of 8 groups, which are numbered in Figure 3. The same process is repeated for $M_{\rm BH}$ and $n_{\rm Edd}$.

We then compute the (variance-weighted) ensemble structure functions for the quasars in each of the 8 groups, using the same methods as in Section 2

5.2 Results for subensembles in $L_{\rm bol}$, $M_{\rm BH}$, and $n_{\rm Edd}$

The results on the r-band SF, grouped by black hole mass, are shown in Figure 4, with the full results for g, r and i against each of $L_{\rm bol}$, $M_{\rm BH}$, and $n_{\rm Edd}$, shown in Figures C3, C4, and C5 respectively. We find that both the amplitude and the slope of the structure function

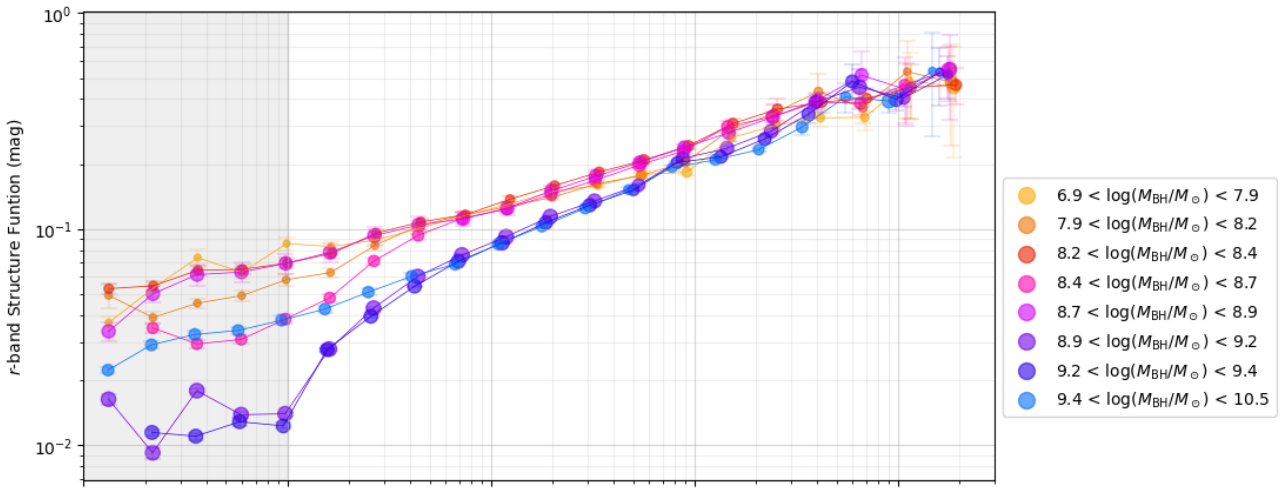

Figure 4. Structure functions of subensembles grouped by black hole mass in the r band. (Full results for all of g, r, and i bands, and for all of $L_{\rm bol}$, $M_{\rm BH}$, and $n_{\rm Edd}$, are shown in Appendix C.) The shaded region represents timescales $\Delta t < 10$ days and is mostly dominated by noise.

changes with each of $L_{\rm bol}$,$M_{\rm BH}$, and $n_{\rm Edd}$. The general sense of the results is that quasars are more variable, and show steeper SF slopes, at lower luminosities, for smaller black hole masses, and for lower values of $n_{\rm Edd}$. Another way to look at the slope result is that quasar variability is more strongly distinguished on short timescales than on long timescales. The clearest version of this general result is shown in Figure 4 which shows the r-band SF grouped by black hole mass. Quasar variability seems to converge towards being towards being *identical* at the longest observed timescales, whereas at shorter timescales, quasars are progressively more distinguished as a function of black hole mass.

The timescale dependence / convergence effect is also present but weaker in the luminosity dependence (Figure C3, **??**), and possibly weakest in the $n_{\rm Edd}$ dependence (Figure C5), depending on wavelength. The amplitude dependence is also clear in all three properties. The luminosity-amplitude effect is consistent with the long-standing result that variability is stronger for lower-luminosity effects. Seeing this effect across a large range of timescales using the SF was first seen by dV05, but only in two broad luminosity ranges. Here we have a cleaner result, and can see the effect marching gradually across luminosity. Our results also confirm and extend those reported by Arévalo et al. (2023), who found that the anti-correlation of variability with black hole mass and Eddington ratio is stronger at short timescales. We agree with their suggestion that this timescale dependence resolves contradictions previously found between different studies.

Although the slope of the SF varies with quasar properties, the SF of each subensemble still seems consistent with a power-law. To quantify our results we have therefore fitted a SPL form, as in eqn XX, to each subensemble in each band. Figure 5 shows the trends of amplitude and slope against each of $L_{\rm bol}$, $M_{\rm BH}$, and $n_{\rm Edd}$. Overall, this confirms the qualitative discussion above - that SF amplitude and slope vary systematically with $M_{\rm BH}$, $L_{\rm bol}$ and $n_{\rm Edd}$. There are however some interesting band-dependent results. The SF slope trend seems to be roughly consistent across g, r and i, with some evidence of anomalous behaviour in i. The SF amplitude is stronger in g than r, and there is marginal evidence that the amplitude in r is stronger than in i.

Of course $M_{\rm BH}$, $L_{\rm bol}$ and $n_{\rm Edd}$ are not independent quantities. It is not clear which property is the primary determinant of variability.

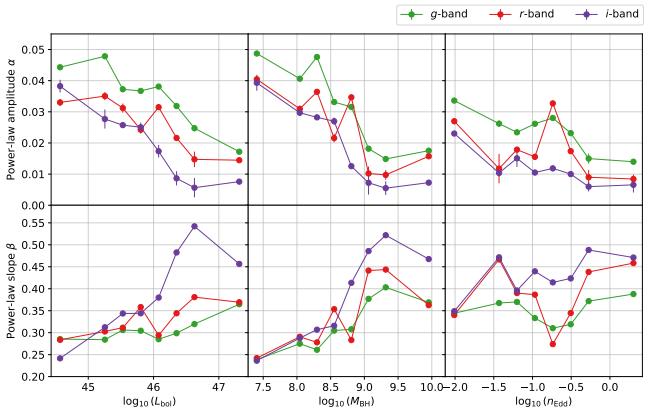

Figure 5. Dependence of SPL amplitude and slope on $L_{\rm bol}$, $M_{\rm BH}$, and $n_{\rm Edd}$, in the g, r and i bands

The black hole mass result does seem clearest. On the other hand, the convergence effect shows that on the longest timescales, quasar variability *does not care* what the black hole mass is.

5.3 Wavelength dependence of the SF

We noted above that the SF amplitude changes from g to r to i. However, the quasars have a range of redshifts, so that the g, r and i bands represent a variety of rest wavelengths. We therefore made further sub-ensemble results by grouping the quasars into ranges of rest wavelength, regardless of observed band. The result is shown in Figure 6. This recovers the well known effect that quasars are more variable in the blue than in the red. However, once again we see differentiation by timescale; the strongest difference is at short timescales - within the scatter, variability does not depend on wavelength for the longest timescales.

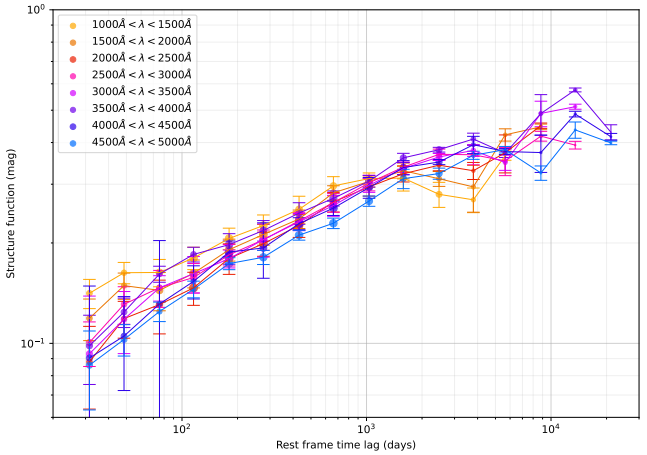

Figure 6. Structure functions of subensembles grouped by rest wavelength.

6 CORRELATION ANALYSIS VERSUS QUASAR PROPERTIES

The results of Section 5 show that variability depends on quasar properties, but that this dependence is a function of timescale. In this section we take a different approach to examining the timescale dependence. Rather than grouping the quasars by properties such as $L_{\rm bol}$ etc, we estimate the SF amplitude for individual quasars, and likewise, using the individual property values, we test how well correlated the amplitude of variability is with that property. We then repeat this calculation for different timescales.

6.1 Calculation methods

For each quasar, we group its $(\Delta m, \Delta t)$ values in a chosen range of Δt. We then use those Δm values to calculate the value of the SF in that Δt range. We then repeat this for different Δt ranges. This results in a very sparse structure function for each quasar. However, this is not a problem, since we will be looking for correlations between values of the structure function on different timescales and quasar properties, rather than plotting the structure function as we have done previously.

For a particular Δt bin, we then calculate the Spearman correlation coefficient, ρ, between quasar properties and the values of the structure function for that bin, SF(Δt). We repeat this process over a set of Δt bins and different quasar properties (luminosity, black hole mass and Eddington ratio). Using luminosity as an example, the Spearman correlation coefficient with SF(Δt) may be expressed as

$$\rho(\Delta t) = \rho\left(L_{\rm bol}, {\rm SF}(\Delta t)\right), \tag{9}$$

with a standard error,

$$\sigma = \sqrt{\frac{1-\rho^2}{n-2}}, \tag{10}$$

where n is the number of points in the bin. The Spearman correlation coefficient can take values $-1 < \rho < 1$, where -1 implies a perfect monotonic negative relationship, $+1$ implies a perfect monotonic positive relationship, and 0 implies no correlation. For each ρ, we also calculate the p-value for a two-sided hypothesis test, whose null hypothesis is that of no ordinal correlation. The p-value roughly indicates the probability of an uncorrelated system that has the same (or greater) value of ρ. The quantity $\rho(\Delta t)$ enables us to quantify the dependence of quasar properties on variability as a function of timescale.

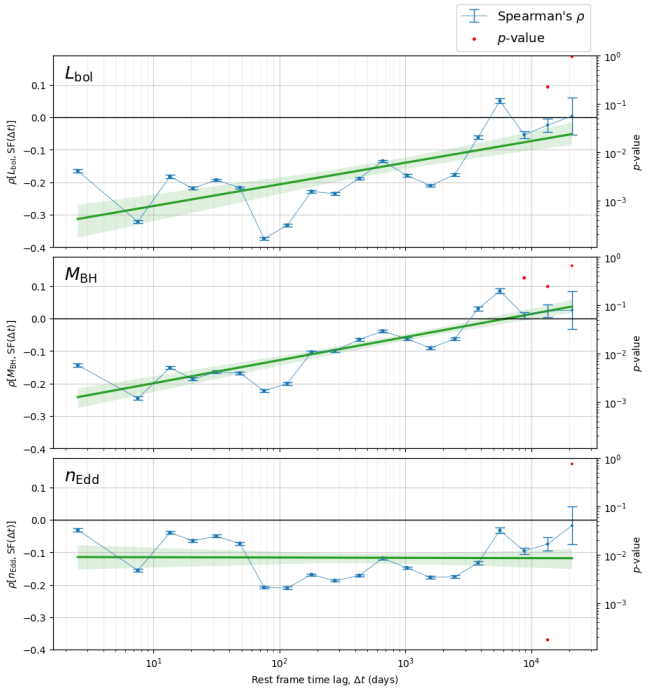

Figure 7. Spearman correlation coefficient between variability amplitude and $L_{\rm bol}$, $M_{\rm BH}$ and $n_{\rm Edd}$ for varying timescales (blue). A line of best fit is overplotted on each panel (green) showing a 2σ confidence interval (shaded green). p-values are shown using the right-hand axis, however, the lower axis limit is set to 10^{-4} and the majority of p-values are well below this limit.

6.2 Correlation Results

Figure 7 shows the Spearman correlation coefficient, $\rho(\Delta t)$, plotted against Δt for luminosity, black hole mass and Eddington ratio. We included the p-value for each calculation of ρ, using a second axis. Note that most of these values are well below $p = 10^{-4}$ and are therefore not present on the plot. For each property, there are an average of $\sim 50,000$ points per bin; however, there are significantly fewer points in the final few bins which is the cause of the larger error bars and higher p-values. The number of points in the final three Δt bins are 9276, 2506, 302, respectively.

These results show that the anticorrelation between bolometric luminosity and variability amplitude depends strongly on the timescale of such variability. On timescales $\Delta t < 10^3$ days, the anticorrelation is strong at $\rho \approx -0.25$, but becomes much weaker on longer timescales and even disappears on timescales of 2×10^4 days. The same anticorrelation is true for black hole mass, but to a lesser degree on shorter timescales. Interestingly, the correlation becomes positive for $\Delta t > 2 \times 10^4$ days, which could explain the positive correlation seen by Wilhite et al. (2008); MacLeod et al. (2010), and Lu et al. (2019). However, since $L_{\rm bol}$ and $M_{\rm BH}$ are themselves correlated, a more detailed analysis is required to decouple these correlations. Such an analysis is certainly possible with 7-DQ, but it is beyond the scope of this paper and will be reserved for a future publication.

The correlation between variability and Eddington ratio is remarkably constant with time-lag, and is scattered around an average value of $\rho = -0.11$. Overall, the correlation is weak, but statistically significant. This persists until timescales of $2{\times}10^4$ days, at which point the correlation disappears, as with luminosity and black hole mass. These are striking results and suggest that on timescales of > 50 years, the

amplitude of variability exhibited by all quasars, irrespective of their properties, is the same.

7 DISCUSSION

We begin by summarising the clearest results:

- The ensemble SF for all quasars is a power law of slope $\beta \sim 0.35$ over four decades of timescale
- The SF is inconsistent with a DRW form, and shows no sign of a long-timescale knee out to ~ 30 year
- On timescales longer than $\sim$ years the SF is asymmetric, in the sense that brightening fluctuations show a different SF shape from dimming fluctuations.
- The slope and the amplitude of the SF depend on all $L_{\rm bol}$, $M_{\rm BH}$, and

vvvv

why not DRW
ensemble of DRWs - fine tuning?
other ways to make SF
overall, on longest timescales

the MH short timescale turn down

8 CONCLUSIONS

ACKNOWLEDGEMENTS

DATA AVAILABILITY

References

Angione R. J., Smith H. J., 1972, in Evans D. S., Wills D., Wills B. J., eds, Proceedings of the International Astronomical Union Symposium Vol. 44, External Galaxies and Quasi-Stellar Objects. p. 171
Arévalo P., Lira P., Sánchez-Sáez P., Patel P., López-Navas E., Churazov E., Hernández-García L., 2023, MNRAS, 526, 6078
Bauer A., Baltay C., Coppi P., Ellman N., Jerke J., Rabinowitz D., Scalzo R., 2009, ApJ, 696, 1241
Cristiani S., Trentini S., La Franca F., Andreani P., 1997, A&A, 321, 123
Hawkins M. R. S., 2002, MNRAS, 329, 76
Helfand D. J., Stone R. P. S., Willman B., White R. L., Becker R. H., Price T., Gregg M. D., McMahon R. G., 2001, AJ, 121, 1872
Hook I. M., McMahon R. G., Boyle B. J., Irwin M. J., 1994, MNRAS, 268, 305
Kelly B. C., Bechtold J., Siemiginowska A., 2009, ApJ, 698, 895
Kelly B. C., Treu T., Malkan M., Pancoast A., Woo J.-H., 2013, ApJ, 779, 187
Kozłowski S., 2016, ApJ, 826, 118
Li Z., McGreer I. D., Wu X.-B., Fan X., Yang Q., 2018, ApJ, 861, 6
Lindsey W. C., Chie C. M., 1976, IEEE Proceedings, 64, 1652
Lu K.-X., et al., 2019, ApJ, 877, 23
MacLeod C. L., et al., 2010, ApJ, 721, 1014
MacLeod C. L., et al., 2012, ApJ, 753, 106
Morganson E., et al., 2014, ApJ, 784, 92
Press W. H., Rybicki G. B., Hewitt J. N., 1992, ApJ, 385, 404
Rakshit S., Stalin C. S., 2017, ApJ, 842, 96
Sánchez-Sáez P., Lira P., Mejía-Restrepo J., Ho L. C., Arévalo P., Kim M., Cartier R., Coppi P., 2018, ApJ, 864, 87
Schmidt K. B., Marshall P. J., Rix H.-W., Jester S., Hennawi J. F., Dobler G., 2010, ApJ, 714, 1194
Sesar B., et al., 2006, AJ, 131, 2801
Simm T., Salvato M., Saglia R., Ponti G., Lanzuisi G., Trakhtenbrot B., Nandra K., Bender R., 2016, A&A, 585, A129
Simonetti J. H., Cordes J. M., Heeschen D. S., 1985, ApJ, 296, 46
Stone Z., et al., 2022, MNRAS, 514, 164
Sumi T., et al., 2005, MNRAS, 356, 331
Vanden Berk D. E., et al., 2004, ApJ, 601, 692
Voevodkin A., 2011, arXiv e-prints, p. arXiv:1107.4244
Wilhite B. C., Brunner R. J., Grier C. J., Schneider D. P., vanden Berk D. E., 2008, MNRAS, 383, 1232
Wu Q., Shen Y., 2022, ApJS, 263, 42
Zuo W., Wu X.-B., Liu Y.-Q., Jiao C.-L., 2012, ApJ, 758, 104
de Vries W. H., Becker R. H., White R. L., Loomis C., 2005, AJ, 129, 615

APPENDIX A: REVIEW OF STRUCTURE FUNCTION DEFINITIONS

Structure functions are a class of functions originally developed for telecommunications engineering in the 1970s (see Lindsey & Chie 1976 and references therein). They provide a robust means to quantify variability of irregular and sparse time series, and became popular with astronomers the following decade. Simonetti et al. (1985) first used structure functions in the context of astronomy, where they applied the first-order structure function to analyse flicker of extragalactic radio sources. Hereafter, we use the term "structure function" to refer to the first order structure function.

Over its 40-year history, different interpretations of the structure function have resulted in an abundance of definitions. In this section, we state and compare some of the most common definitions and hope this may be useful to readers navigating the literature. A through review of structure function definitions in the literature can be found in Kozłowski (2016).

In its most general form, the structure function of a light curve is the RMS of the magnitude differences $\Delta m = m(t_j) - m(t_i)$ evaluated at times t_j and t_i, separated by a time-lag $\Delta t = t_j - t_i$. Simonetti et al. (1985) define the structure function as:

$$\mathrm{SF}_{\rm obs}(\Delta t) = \sqrt{\frac{1}{N(\Delta t)} \sum_{j<i} \Delta m_{ij}^2}, \tag{Si85}$$

where we have used the 'obs' to be explicit that this is the total observed structure function. Sumi et al. (2005) and Hook et al. (1994) instead define the SF as the median of magnitude changes,

$$\mathrm{SF}(\Delta t) = \mathrm{med}\left(\Delta m_{ij}^2\right), \tag{Su05}$$

with the latter using the modulus instead of the square of Δm pairs. Vanden Berk et al. (2004) estimate intrinsic variability by subtracting photometric noise,

$$\mathrm{SF}(\Delta t) = \left\langle \sqrt{\frac{\pi}{2}} \left|\Delta m_{ij}\right| - \left\langle \sigma^2 \right\rangle \right\rangle, \tag{VB04}$$

where angled brackets denote a mean average. Bauer et al. (2009) used a similar definition,

$$\mathrm{SF}(\Delta t) = \sqrt{\left\langle \Delta m_{ij}^2 \right\rangle - \left\langle \sigma^2 \right\rangle}, \tag{B09}$$

however, both definitions subtract $\langle \sigma^2 \rangle$ instead of the expected $2\langle \sigma^2 \rangle$, which leads to a flatter SF. The equation

$$\mathrm{SF}(\Delta t) = \left\langle \sqrt{\frac{\pi}{2}} \left|\Delta m_{ij}\right| - \sqrt{\sigma_i^2 + \sigma_j^2} \right\rangle \tag{Sc10}$$

from Schmidt et al. (2010) seems to subtract too much noise, since σ has not also been scaled by $\pi/2$. MacLeod et al. (2012) uses the

interquartile range (IQR) between 25% and 75% of the Δm distribution, in order to be robust against outliers,

$$\mathrm{SF}(\Delta t) = 0.741 \times \mathrm{IQR}(\Delta m),, \tag{M12}$$

however, they do not subtract photometric noise. Kozłowski (2016) attempts to remove this photometric noise with the definition:

$$\mathrm{SF}(\Delta t) = 0.741 \times \sqrt{\mathrm{IQR}(\Delta m) - \mathrm{IQR}(n)}, \tag{K16}$$

where $\mathrm{IQR}(n)$ is the IQR of the Δm distribution of the shortest observed time-lags, i.e., the IQR of the photometric noise.

A plethora of definitions causes problems with interpretations and comparisons, and therefore it is important to adopt one system. We use the following definition to approximate the intrinsic structure function,

$$\mathrm{SF}_{\mathrm{int}}(\Delta t) = \sqrt{\frac{1}{N(\Delta t)} \sum_{j<i} (\Delta m_{ij}^2 - \sigma_i^2 - \sigma_j^2)}, \tag{A1}$$

where the sum runs over the $N(\Delta t)$ epochs such that $t_j - t_i = \Delta t$. This definition was originally proposed by Press et al. (1992) and is deemed the most correct way to estimate structure functions by Kozłowski (2016).

APPENDIX B: STRUCTURE FUNCTION: MAGNITUDES OR FLUXES?

When the structure function was first introduced into the context of astronomy by Simonetti et al. (1985), it was defined in terms of fluxes. Hook et al. (1994) later defined it in terms of magnitudes, without justification for the switch, which was adopted by all subsequent studies in the field. Since magnitudes are logarithmic, symmetric variations in flux will lead to asymmetric variations in magnitude. For small perturbations in magnitude, this asymmetry is negligible. However, large magnitude changes could introduce significant bias. Since there do not seem to be any studies which measure this effect, we simulated a simple toy model to approximate the extent of the bias.

We used a DRW process ($\mathrm{SF}_\infty = 5 \times 10^{-6}$ Jy, $\mu = 10^{-5}$ Jy, $\tau_{\mathrm{DRW}} = 10^3$ days) to simulate the flux output of a quasar and calculated the structure function using fluxes. We chose these values for SF_∞ and μ as they correspond to a 21.4 mag quasar with $\mathrm{SF}_\infty \approx 0.5$ mag which are typical values for our 7-DQ quasars. We found that τ_{DRW} had little effect on the bias, so we picked a reasonable value of 10^3 days. We converted flux, f, to magnitudes, m, using the relation,

$$m = -2.5 \log_{10}(f) + 8.9, \tag{B1}$$

and calculated the corresponding structure function using magnitudes. We computed the fractional difference between these two structure functions for each Δt bin in a set of 30 logarithmically spaced Δt bins over the range $10 < \Delta t < 3 \times 10^4$ days. We computed the mean and standard deviation of these fractional differences and repeated the process for 50 runs. We found the average of these means and standard deviations to be 5.51% and 5.53%, respectively. While this is quite a rudimentary calculation, the average fractional difference of $\sim$5% is small enough to conclude that the use of magnitudes in structure function calculations does not introduce significant asymmetric bias.

APPENDIX C: COMPLETE SF RESULTS

In the main body of text we illustrated we key results on the SF in specific wavebands and subensembles. Here we collect figures illustrating all the SF calculations referred to.

This paper has been typeset from a TEX/LATEX file prepared by the author.

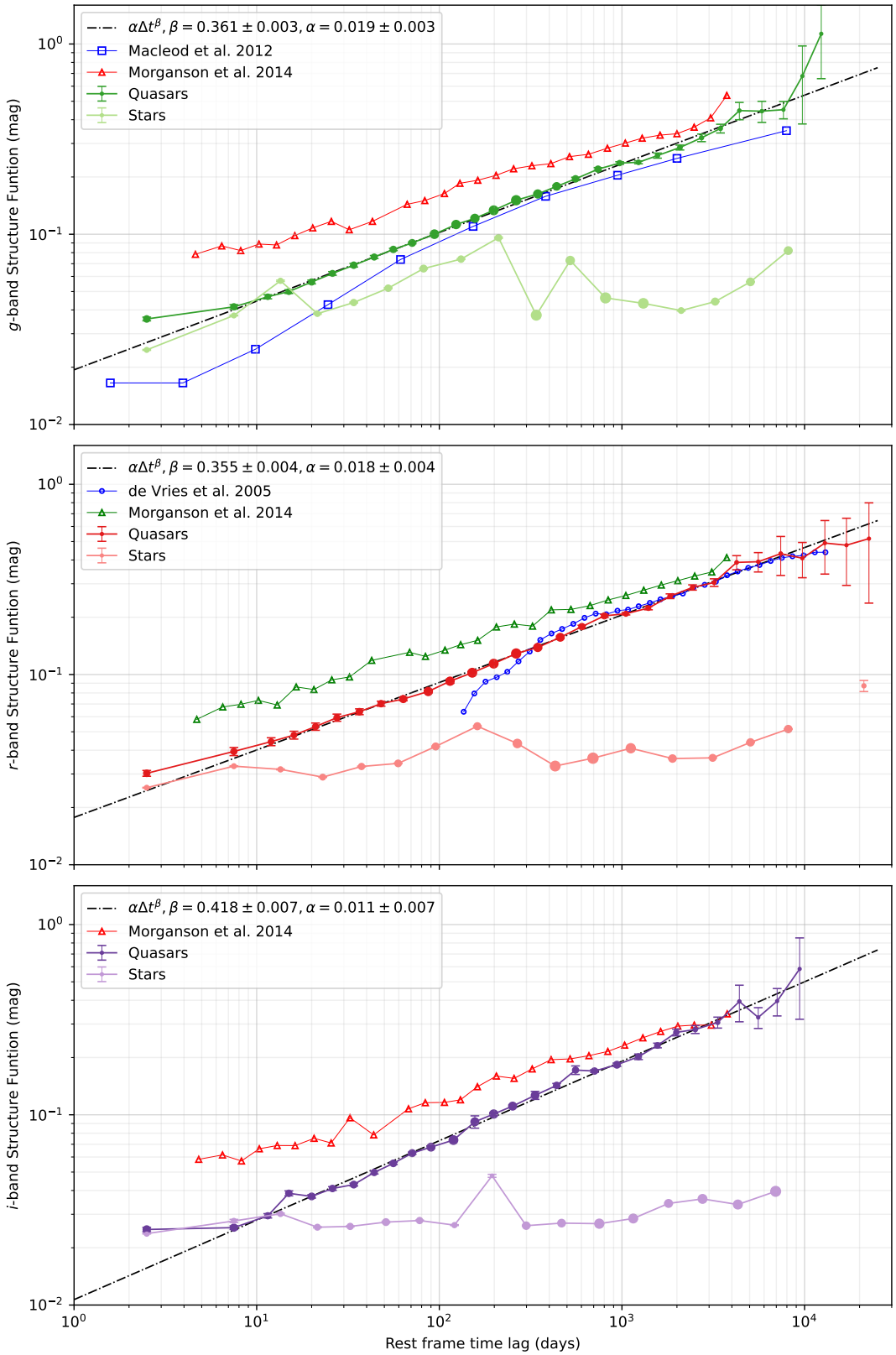

Figure C1. Ensemble structure function for the quasars and stars in the g, r and i bands. The size of the points represents the relative number of points in the bin. The black dot-dashed line represents an SPL fit to the quasar structure function data points for $\Delta t > 10$ days, with the slope shown in the legend. Comparison data from MacLeod et al. 2012, de Vries et al. 2005, and Morganson et al. 2014 are overplotted. A few points are omitted for the ensemble star structure function, as the photometric errors are greater than the observed variability.

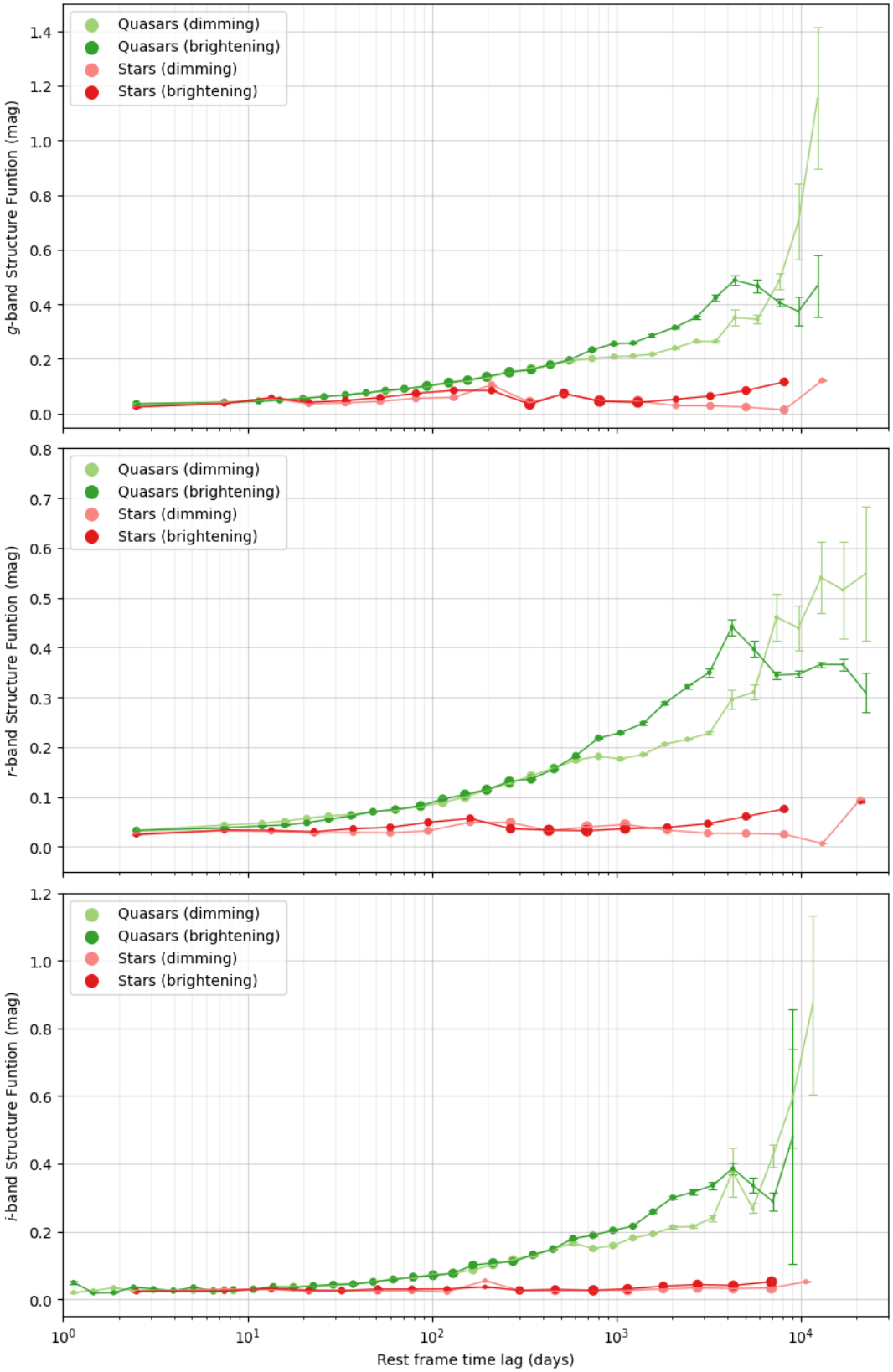

Figure C2. Positive and negative structure functions plotted for the quasar and star population in the 6, A and 8 bands. Fluctuations that involve brightening are illustrated with opaque points, while those representing dimming are in translucent points.

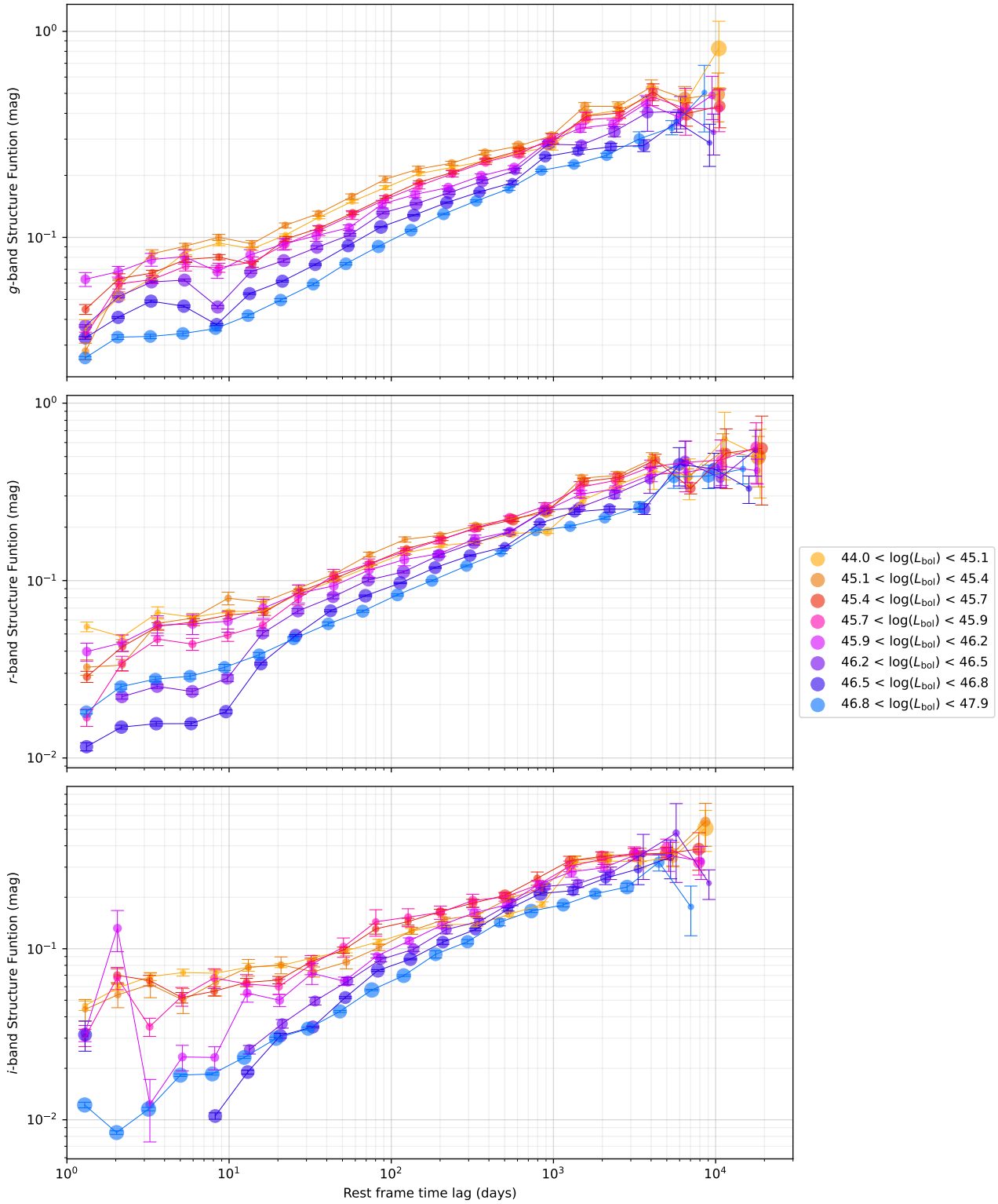

Figure C3. Structure functions of subensembles grouped by bolometric luminosity in the g, r and i bands. The shaded region represents timescales $\Delta t < 10$ days and is mostly dominated by noise.

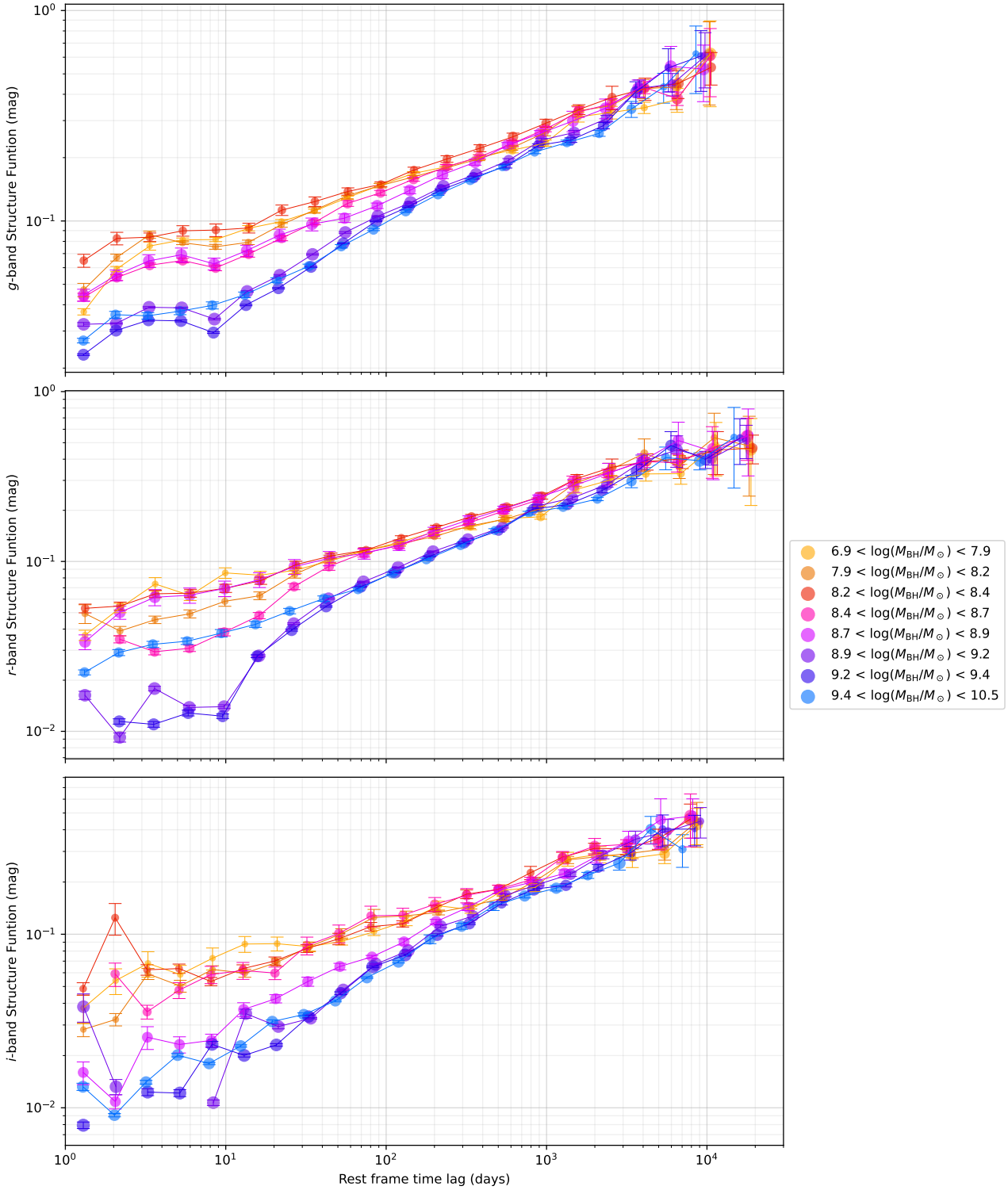

Figure C4. Structure functions of subensembles grouped by black hole mass in the g, r and i bands. The shaded region represents timescales $\Delta t < 10$ days and is mostly dominated by noise.

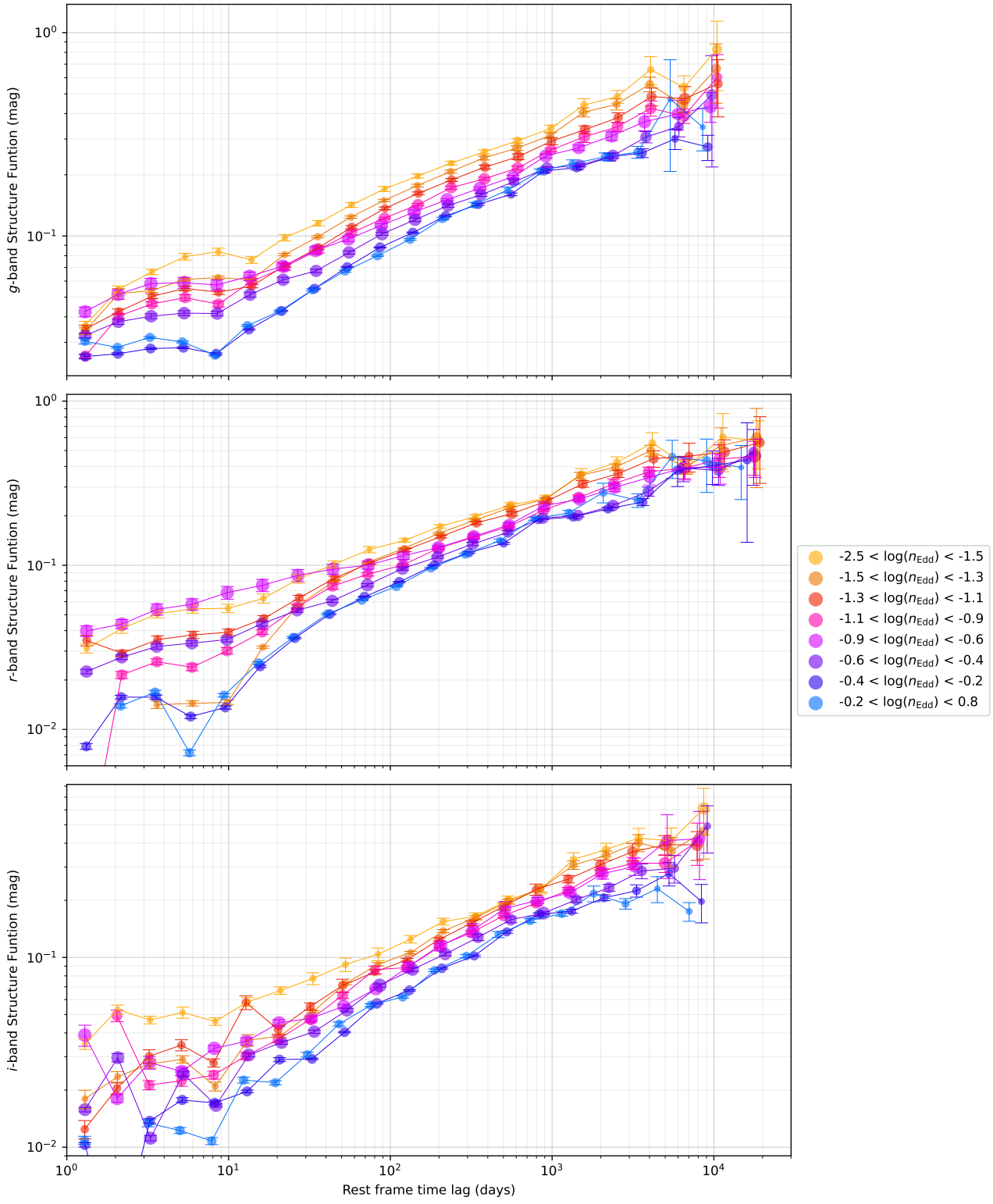

Figure C5. Structure functions of subensembles grouped by Eddington ratio in the g, r and i bands. The shaded region represents timescales $\Delta t < 10$ days and is mostly dominated by noise.